Inorg. Chem. **2004**, *43*, 6969–6978

Electrochemical, Spectral, and Computational Studies of Metalloporphyrin Dimers Formed by Cation Complexation of Crown Ether Cavities†

Raghu Chitta, Lisa M. Rogers, Amber Wanklyn, Paul A. Karr, Pawan K. Kahol, Melvin E. Zandler, and Francis D'Souza*

Department of Chemistry, Wichita State University, 1845 Fairmount, Wichita, Kansas 67260-0051

Received March 3, 2004

The effect on the electrochemical oxidation and reduction potentials of 5,10,15,20-tetrakis(benzo-15-crown-5)-porphyrin (TCP) and its metal derivatives (MTCP; M = Mg(II), VO(IV), Co(II), Ni(II), Cu(II), Zn(II), Pd(II), Ag(II)) upon potassium ion induced dimerization of the porphyrins was systematically performed in benzonitrile containing 0.1 M $(TBA)ClO_4$ by differential pulse voltammetry technique. The HOMO–LUMO energy level diagram constructed from the electrochemical data revealed destabilization of the HOMO level and stabilization of the LUMO level upon dimer formation while such a perturbation was larger for the HOMO level than the LUMO level. The geometry and electronic structure of a representative ZnTCP and its dimer, $K_4(ZnTCP)_2$, were evaluated by the ab initio B3LYP method utilizing a mixed basis set of 3-21G(*) for Zn, K, O, and N and STO-3G for C and H. The inter-porphyrin ring distance of the dimer calculated from the optimized geometry agreed with the spectroscopically determined one, and the calculated HOMO and LUMO frontier orbitals revealed delocalization on both of the porphyrins rings. The metal–metal distances calculated from the triplet ESR spectra of the K^+ induced porphyrin dimers bearing paramagnetic metal ions in the cavity followed the trend Cu–Cu < VO–VO < Ag–Ag. However, the spectral shifts resulting from the exciton coupling of the interacting porphyrin π-systems revealed no specific trend with respect to the metal ion in the porphyrin cavity. Additionally, linear trends in the electrochemically measured HOMO–LUMO gap and the energy corresponding to the most intense visible band of both MTCP and $K_4(MTCP)_2$ were observed. A reduced HOMO–LUMO gap predicted for the dimer by B3LYP/(3-21G(*), STO-3G) calculations was confirmed by the results of optical absorption and electrochemical studies.

Introduction

Self-assembled supramolecular metalloporphyrins have been the subject of increasing investigation because of their importance as model compounds to mimic biological functions and as materials for constructing electrocatalytic, electronic, and optical devices.[1] In this regard, porphyrin dimers are one of the most widely studied classes of compounds since they mimic the primary donor entity of the bacterial photosynthetic reaction center and act as electrocatalysts for a direct four-electron reduction of dioxygen to water.[2] Several covalently and a few noncovalently linked porphyrin dimers, varying in their distance and orientation, have been elegantly designed and studied to unravel the distance and orientation factors of the two interacting porphyrin macrocycles on their physicochemical

* Author to whom correspondence should be addressed. E-mail: Francis.DSouza@wichita.edu.

† This paper is dedicated to the memory of Prof. Bhaskar G. Maiya (1956−2004).

(1) *Supramolecular Chemistry: Concepts and Perspectives*; Lehn, J.-M., Ed.; VCH: New York, 1995. (b) *Molecular Switches*; Feringa, B. L., Ed.; Wiley-VCH GmbH: Weinheim, Germany, 2001. (c) *Introduction of Molecular Electronics*; Petty, M. C., Bryce, M. R., Bloor, D., Eds.; Oxford University Press: New York, 1995. (d) *Molecular Electronic-Science and Technology*; Aviram, A., Ed.; Engineering Foundation: New York, 1989.

(2) (a) *The Photosynthetic Reaction Center*; Deisenhofer, J., Norris, J. R., Eds.; Academic Press: San Diego, CA, 1993. (b) El-Kobbani, O.; Chang, C. H.; Tiede, D.; Norris, J.; Schiffer, M. *Biochemistry* **1991**, *30*, 5361. (c) Fromme, P. *Curr. Opin. Struct. Biol*. **1996**, *6*, 473. (d) *The Porphyrin Handbook*; Kadish, K. M., Smith, K. M., Guilard, R., Eds.; Academic Press: Burlington, MA, 2000; Vol. 1. (e) Chang, C. K.; Abdalmuhdi, I. *Angew. Chem., Int. Ed. Engl*. **1984**, *23*, 164. (f) Deng, Y.; Chang, C. J.; Nocer, D. G. *J. Am. Chem. Soc*. **2000**, *122*, 410. (g) Collman, J. P.; Wagenknecht, P. S.; Hutchison, J. E. *Angew. Chem., Int. Ed. Engl*. **1994**, *33*, 1537. (h) D'Souza, F.; Hsieh, Y.-Y.; Deviprasad, G. R. *Chem. Commun*. **1998**, 1027. (i) Fukuzumi, S.; Okamoto, K.; Gros, C. P.; Guilard, R. *J. Am. Chem. Soc*. **2004**, *126*, 10441.

10.1021/ic0497228 CCC: $27.50
Published on Web 10/05/2004

Chart 1. Structure of 5,10,15,20-Tetrakis(benzo-15-crown-5)porphyrin (TCP) and Its Metal Derivatives (MTCP)[a]

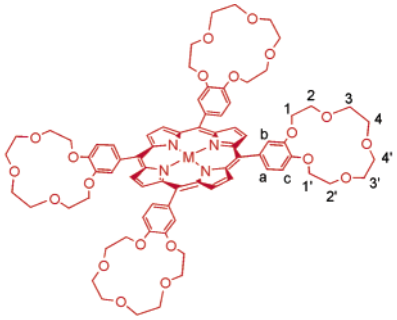

TCP; M = 2H
MTCP; M = Mg(II), VO(IV), Co(II), Ni(II), Cu(II), Zn(II), Pd(II), Ag(II)

[a] The numbering of the phenyl and ethoxy protons is shown.

properties.[2d−i] Among the noncovalently linked porphyrin dimers, the dimers formed by cation (K^+, NH_4^+, Cs^+, Ba^{2+}) complexation of 5,10,15,20-tetrakis(benzo-15-crown-5)porphyrin (TCP) and their metal derivatives (MTCP), synthesized by Thanabal and Krishnan, are one of the attractive classes of compounds (Chart 1).[3,4] The structure of the dimers were deduced from the stoichiometry of the dimerization reaction and from ESR and ENDOR studies of the Cu(II) and VO(IV) metallated porphyrins.[3−6] The optical and emission properties of the cation-induced supramolecular dimers were found to be different from those of the monomeric entities. From these studies and from space-filling molecular modeling it was concluded that the two porphyrin rings in the dimer are stacked through a common symmetry axis normal to the planes, with an interplanar distance of ~4.2 Å.[3−6]

Since the first report on crown ether appended porphyrins in 1982,[3] different types of crown ether appended porphyrins varying in the size and position of the crown ether cavities and, in some instances, having additional peripheral substituents on the porphyrin ring have been elegantly designed and studied by various research groups.[7−15] Interesting sensor and catalytic applications have also been sought from these studies. Some of the interesting examples of crown ether appended porphyrins include the following: a supramolecular cup-and-ball porphyrin−C_{60} donor−acceptor conjugate reported by Solladie et al.[7] for the study of light-induced electron transfer; a bis(pyridyl) crown-capped porphyrin for cofacial anchoring of the porphyrins;[8] crown ether appended N-confused porphyrin with enhanced face-to-face dimerization ability;[9] a porphyrin-based peptide receptor by Sirish et al.;[10] an ion-pair recognizing ditopic zinc porphyrin−crown ether conjugate;[11] a series of crown ether-annulated porphyrins serving as ion channels by Murashima et al.;[12] a crown-expanded porphyrin (sapphyrin) acting as a receptor for concurrent complexation of both anionic and cationic substances by Sessler et al.;[13] a novel porphyrin covalently bonded to a redox-active crown ether by Kurreck and coworkers;[14] a porphyrin−crown ether based co-receptor molecule by Hamilton et al.[15] Several additional studies have also been performed to visualize physicochemical properties of the porphyrin−crown ether molecular systems.[16,17]

Understanding the redox behavior of the cation-induced crown ether appended porphyrin dimer is important since it provides information about the relative energies of the highest occupied molecular orbital (HOMO), and the lowest unoccupied molecular orbital (LUMO), as compared to the monomer entity. In this regard the only study on the electrochemistry of cation-induced crown ether porphyrin dimers reported by Maiya and Krishnan[18] was restricted to the anodic electrochemistry because of the utilized solvent and electrolyte medium. As a result, a complete picture of the relative HOMO and LUMO energies of the porphyrin dimers could not be obtained. Since such information is the key in the newly emerging field of organic and electrode materials, especially for the development of nanodevices through self-assembled supramolecular structures,[1,2] in this study, we have re-investigated the electrochemical behavior of cation induced crown ether porphyrin dimers by choosing a solvent and electrolyte medium that enables both the anodic and cathodic electrochemistry of both the porphyrin monomers and dimers to be probed. Here, the free-base porphyrin, TCP, and its Mg(II), VO(IV), Co(II), Ni(II), Cu(II), Zn(II), Pd(II), and Ag(II) metal derivatives were synthesized and studied to visualize the effect of the metal ion in the porphyrin cavity. In this metalloporphyrin series, the Pd(II) and Ag(II) crown ether appended porphyrins had not been previously investigated. Additionally, the structure and electronic properties of the crown ether zinc porphyrin monomer and cation complexation induced zinc porphyrin dimer were modeled by ab initio B3LYP/(3-21G(*), STO-3G) methods. The computed parameters were compared with

(3) Thanabal, V.; Krishnan, V. *J. Am. Chem. Soc.* **1982**, *104*, 3643.
(4) Thanabal, V.; Krishnan, V. *Inorg. Chem.* **1982**, *21*, 3606.
(5) van Willigen, H.; Chandrashekar, T. K. *J. Am. Chem. Soc.* **1986**, *108*, 709.
(6) Chandrashekar, T. K.; van Willigen, H.; Ebersole, M. *J. Phys. Chem.* **1985**, *89*, 3453.
(7) Solladie, N.; Walther, M. E.; Gross, M.; Duarte, F.; Teresa, J.; Bourgogne, C.; Nierengarten, J.-F. *Chem. Commun.* **2003**, 2412.
(8) Ruzie, C.; Michaudet, L.; Boitrel, B. *Tetrahedron Lett.* **2002**, *43*, 7423.
(9) Shinmori, H.; Furuta, H.; Osuka, A. *Tetrahedron Lett.* **2002**, *43*, 4881.
(10) Sirish, M.; Schneider, H.-J. *Chem. Commun.* **1999**, 907.
(11) Kim, Y.-H.; Hong, J.-I. *Chem. Commun.* **2002**, 512.
(12) Murashima, T.; Uchihara, Y.; Wakamori, N.; Uno, H.; Ogawa, T.; Ono, N. *Tetrahedron Lett.* **1996**, *37*, 3133.
(13) Sessler, J. L.; Brucker, E. A. *Tetrahedron Lett.* **1995**, *36*, 1175.
(14) Sun, L.; von Gersdorff, J.; Niethammer, D.; Tian, P.; Kurreck, H. *Angew. Chem., Int. Ed. Engl.* **1994**, *33*, 2318.
(15) Hamilton, A.; Lehn, J. M.; Sessler, J. L. *J. Am. Chem. Soc.* **1986**, *108*, 5158.
(16) (a) Langford, S. J.; Lau, V.-V.; Lee, M. A. P.; Lygris, E. *J. Porphyrins Phthalocyanines* **2002**, *6*, 748. (b) Shinmori, H.; Yasuda, Y.; Osuka, A. *Eur. J. Org. Chem.* **2002**, *7*, 1197. (c) Sirish, M.; Chertkov, V. A.; Schneider, H.-J. *Chem.—Eur. J.* **2002**, *8*, 1181. (d) Duggan, S. A.; Fallon, G.; Langford, S. J.; Lau, V.-L.; Satchell, J. F.; Paddon-Row, M. N. *J. Org. Chem.* **2001**, *66*, 4419. (e) Shinmori, H.; Osuka, A. *Tetrahedron Lett.* **2000**, *41*, 8527. (f) Michaudet, L.; Richard, P.; Boitrel, B. *Tetrahedron Lett.* **2000**, *41*, 8289. (g) Iwata, S.; Suzuki, N.; Shirakawa, M.; Tanaka, K. *Supramolecular Chem.* **1999**, *11*, 135.
(17) (a) Diskin-Posner, H.; Krishna Kumar, R.; Goldberg, I. *New. J. Chem.* **1999**, *23*, 885. (b) Gunter, M. J.; Jeynes, T. P.; Johnston, J. R.; Turner, P.; Chen Z. *J. Chem. Soc., Perkin Trans. 1* **1998**, 1945. (c) Gibney, B. R.; Wang, H.; Kampf, J. W.; Pecoraro, V. L.; Willard, H. *Inorg. Chem.* **1996**, *35*, 6184. (d) Krishnan, V.; Batova, E. E.; Shafirovich, V. Y. *J. Photochem. Photobiol., A* **1994**, *84*, 233. (e) Kral, V.; Pankova, M.; Guenterova, J.; Belohradsky, M.; Anzenbacher, P., Jr. *Chem. Commun.* **1994**, *59*, 639. (f) Gunter, M. J.; Johnston, M. R. *Tetrahedron Lett.* **1992**, *33*, 1771.
(18) Maiya, G. B.; Krishnan, V. *Inorg. Chem.* **1985**, *24*, 3253.

Table 1. UV−Visible Absorption Data on Crown Ether Appended Porphyrins and Their Potassium Ion Induced Dimers

compd	ionic radius, Å[a]	Soret band, nm	Q-bands, nm	$\Delta\bar{\nu}_{Soret}$, cm^{-1}	$\Delta\bar{\nu}_{visible}$, cm^{-1}
TCP		429.4	521.4, 559.1, 595.4, 654.0		
TCP + K^+		414.0	521.4, 569.4, 602.7, 662.6	871	323[b]
MgTCP	0.71	434	569, 610		
MgTCP + K^+		419	573, 615	854	105
VOTCP	0.67	437.0	553.6, 593.0		
VOTCP + K^+		428.6	564.6, 616.5	452	352
CoTCP	0.72	423.0	534.0		
CoTCP + K^+		411.0	538.5	692	156
NiTCP	0.63	426.0	532.6		
NiTCP + K^+		412.0	539.1	799	227
CuTCP	0.71	426.0	543.5, 583.0		
CuTCP + K^+		414.5	551.6, 589.0	649	267
ZnTCP	0.74	434.0	561.0, 603.0		
ZnTCP + K^+		417.0	562.1, 602.0	940	36
PdTCP	0.78	426.5	528.0, 563.5		
PdTCP + K^+		416.0	535.5, 571.0	588	264
AgTCP	0.93	436.5	546.0, 583.5		
AgTCP + K^+		426.0	554.0, 593.0	566	266

[a] From ref 23. [b] Spectral shift calculated for the 559.1 nm of TCP and 594.5 nm of TCP + K^+ complex.

that obtained from electrochemical, optical absorption, and ESR methods.

Experimental Section

The reagents used in the syntheses work were of reagent grade quality from Aldrich (Milwaukee, WI). Benzonitrile (in sure seal bottle), potassium tetrakis(4-chlorophenyl)borate (Aldrich), and tetrabutylammonium perchlorate, (TBA)ClO_4 (Fluka), were utilized for both electrochemical and spectral investigations. The syntheses of TCP and MTCP were carried out according to literature procedures[3,4] with some modifications. All of the compounds were freshly purified prior to the spectral and electrochemical measurements using chromatography methods.

Syntheses of Crown Ether Appended Free-Base Porphyrin and Metalloporphyrins. 4′-Formylbenzo-15-crown-5 (1). The title compound was synthesized according to Hyde et al.[19] Phosphoryl chloride (1.22 mL, 2.042 g, 0.0133 mol) was added to *N*-methylformanilide (1.643 mL, 1.8 g, 0.0133 mol), and the resulting mixture was stirred for 20 min. Benzo-15-crown-5 (1.7 g, 0.00634 mol) was then added, and the mixture was stirred at 90 °C for 4 h. The resulting dark brown mixture was cooled and extracted in chloroform. The chloroform was removed under reduced pressure, and the residual brown oil in ethanol solution (5 mL) was added to a solution of $NaHSO_3$ (10 g, 0.96 mol) in a mixture of water (50 mL) and ethanol (40 mL). The resulting solution was warmed and stirred to obtain the sodium hydrogen sulfite adduct of the product as a heavy white precipitate. The precipitate was collected and suspended in a mixture of water (12 mL) and chloroform (6 mL) at 0 °C, and concentrated H_2SO_4 (12 mL) was added carefully to the stirred suspension until all the solid had dissolved. The chloroform layer was separated, the aqueous layer was extracted with chloroform, and the combined extracts were evaporated under reduced pressure. The resulting oil was dissolved in a boiling mixture of 2-propanol and light petroleum. The required product was crystallized on cooling. Yield: ∼50%. ^{1}H NMR in $CDCl_3$ (δ, ppm): 9.83 (s, 1H), 7.42−7.47 (d,d, 1H), 7.38 (d, 1H), 6.94 (d, 1H), 4.23−4.18 (m, 4H), 3.96−3.89 (m, 4H), 3.79−3.74 (m, 4H).

(19) Hyde, E. M.; Shaw, B. L.; Shepherd, I. *J. Chem. Soc., Dalton Trans.* **1978**, 1696.

5,10,15,20-Tetrakis(benzo-15-crown-5)porphyrin, TCP (2). This was synthesized according to Thanabal and Krishnan[3] with some modifications. A mixture of 4′-formylbenzo-15-crown-5 (600 mg, 2.1 mmol) and pyrrole (166.9 mg, 2.1 mmol) in refluxing propionic acid was refluxed for 3 h. The crude product was purified on a basic alumina column with chloroform as eluent. Yield: ∼5%. ^{1}H NMR in $CDCl_3$ (δ, ppm): 8.88 (s, 8H, β-pyrrole-H), 7.78−7.68 (m, 8H, a,b-phenyl-H), 7.2 (d, 4H, c-phenyl-H), 4.46−4.38 (m, 8H, 1 ether-H), 4.3−4.24 (m, 8H, 1′ ether-H), 4.13−4.06 (m, 8H, 2 ether-H), 3.98−3.93 (m, 8H, 2′ ether-H), 3.92−3.82 (m, 32H, 3,3′,4,4′ ether-H), −2.78 (s, br, 2H, imino-H). See Table 1 for UV−vis data in benzonitrile.

ZnTCP (3). The free-base porphyrin **2** (20 mg, 0.015 mmol) was dissolved in $CHCl_3$ (10 mL), a saturated solution of zinc acetate in methanol was added to the solution, and the resulting mixture was refluxed for 2 h. The course of the reaction was followed spectrophotometrically by monitoring the disappearance of the 521.5 nm band of TCP. At the end, the reaction mixture was washed with water and dried over anhydrous Na_2SO_4. Chromatography on basic alumina column using $CHCl_3$ as eluent gave the title compound. Yield: 18 mg, 0.013 mmol, 90%. ^{1}H NMR in $CDCl_3$ (δ, ppm): 8.96 (s, 8H, β-pyrrole-H), 7.74−7.66 (m, 8H, a,b-phenyl-H), 7.12 (d, 4H, c-phenyl-H), 4.32−4.22 (m, 8H, 1 ether-H), 4.13−3.98 (m, 8H, 1′ ether-H), 3.92−3.89 (m, 8H, 2 ether-H), 3.74−3.38 (m, 40H, 2′,3,3′,4,4′ ether-H). See Table 1 for UV−vis data in benzonitrile.

NiTCP (4). This compound was prepared by reacting **2** with nickel(II) acetate according to the general procedure outlined above for ZnTCP **(2)**. Yield: ∼95%. ^{1}H NMR in $CDCl_3$ (δ, ppm): 8.78 (s, 8H, β-pyrrole-H), 7.3−7.21 (m, 8H, a,b-phenyl-H), 7.2−7.12 (m, 4H, c-phenyl-H), 4.42−4.36 (m, 8H, 1 ether-H), 4.24−4.18 (m, 8H, 1′ ether-H), 4.1−4.05 (m, 8H, 2 ether-H), 3.97−3.91 (m, 8H, 2′ ether-H), 3.9−3.8 (m, 32H, 3,3′,4,4′ ether-H). UV−vis in benzonitrile ($\lambda_{max,}$ nm): 426 and 532.5.

PdTCP (5). This compound was prepared by reacting **2** with palladium(II) acetate according to the general procedure outlined above for ZnTCP **(2)** followed by chromatographic purification on basic alumina column. Yield: ∼70%. ^{1}H NMR in $CDCl_3$ (δ, ppm): 8.85 (s, 8H, β-pyrrole-H), 7.74−7.64 (m, 8H, a,b-phenyl-H), 7.21(d, 4H, c-phenyl-H), 4.47−4.4 (m, 8H, 1 ether-H), 4.27−

4.21 (m, 8H, 1′ ether-H), 4.14−4.07 (m, 8H, 2 ether-H), 3.98−3.93 (m, 8H, 2′ ether-H), 3.92 (m, 32H, 3,3′,4,4′ ether-H). See Table 1 for UV−vis data in benzonitrile.

CoTCP (6). This compound was prepared by reacting **2** with cobalt(II) acetate followed by chromatographic separation on a basic alumina column using $CHCl_3$ as eluent. Yield: ∼90%. ^{1}H NMR in $CDCl_3$ (δ, ppm): 16.5−15.6 (s, br, 8H, β-pyrrole-H), 13.2−12.4 (m, 8H, a,b-phenyl-H), 9.4 (s, 4H, c-phenyl-H), 5.56−5.52 (m, 8H, 1 ether-H), 5.5−5.6 (m, 8H, 1′ ether-H), 5.0−4.56 (m, 8H, 2 ether-H), 4.52−4.15 (m, m, 40H, 2′,3,3′,4,4′ ether-H). See Table 1 for UV−vis data in benzonitrile.

AgTCP (7). This compound was prepared from porphyrin **2** and silver(II) acetate according to the procedure outlined above for ZnTCP **(2)**. Yield: ∼80%. See Table 1 for UV−vis data in benzonitrile.

CuTCP (8). This compound was prepared from porphyrin **2** and copper(II) acetate according to the procedure outlined above for ZnTCP **(2)**. Yield: ∼85%. See Table 1 for UV−vis data in benzonitrile.

VOTCP (9). This compound was prepared by refluxing $VOSO_4$ and porphyrin **2** in DMF under N_2 for 30 h.[3] The progress of the reaction was followed spectrophotometrically. The metalated derivative was purified by using a basic alumina column. Yield: ∼80%. See Table 1 for UV−vis data in benzonitrile.

MgTCP (10). This was prepared according to a general procedure developed by Lindsey and Woodford[20] for Mg porphyrin synthesis. A sample of 10 mg (0.00727 mmol) of TCP was dissolved in 10 mL of CH_2Cl_2. Then 0.0405 mL (0.2908 mmol) of triethylamine was added followed by 37.55 mg (0.1454 mmol) of $MgBr_2{\cdot}O(Et)_2$. The mixture was stirred for 20 min at room temperature. The course of the reaction was monitored by absorption spectroscopy. The mixture was diluted with 20 mL of CH_2Cl_2, washed with 5% $NaHCO_3$, and dried over anhydrous Na_2SO_4, and the filtrate was evaporated. Chromatography on basic alumina column with $CHCl_3$ as eluent yielded residual TCP. Elution with ethyl acetate−methanol (95:5) yielded a greenish pink fraction of the desired compound. Yield: ∼80%. ^{1}H NMR in $CDCl_3$ (δ, ppm): 8.96 (s, 8H, β-pyrrole-H), 7.74−7.55 (m, 8H, phenyl-H), 7.12 (d, 4H, phenyl-H), 4.5−4.3 (m, 8H, ether-H), 4.25−4.0 (m, 8H, ether-H), 3.95−3.8 (m, 8H, ether-H), 3.8−3.6 (m, 40H, ether-H). See Table 1 for UV−vis data in benzonitrile.

Instrumentation. The UV−visible spectral measurements were carried out with a Shimadzu model 1600 UV−visible spectrophotometer. The ^{1}H NMR studies were carried out on a Varian 400 MHz spectrometer. Tetramethylsilane (TMS) was used as an internal standard. Cyclic voltammetry (CV) and differential pulse voltammetry (DPV) were recorded on a EG&G model 263A potentiostat/galvanostat using a three-electrode system. A platinum button or glassy carbon electrode was used as the working electrode. A platinum wire served as the counter electrode, and Ag/AgCl or Ag/Ag^+ was used as the reference electrodes. A ferrocene/ferrocenium redox couple was used as an internal standard for the measured redox potentials. All the solutions were purged prior to electrochemical measurements using nitrogen gas. The ESR spectra were recorded on a Bruker X-band spectrometer at 120 K.

The computational calculations were performed with the GAUSSIAN 03 (revision B-04)[21] software package on high-speed computers. The graphics of HOMO and LUMO coefficients were generated with the help of GaussView-03 software.

Results and Discussion

In this study, we have utilized benzonitrile as the solvent of choice for both spectral and electrochemical studies since this solvent provides good spectral coverage (280−1100 nm) and a good potential window (+2 to −2 V) to probe both anodic and cathodic electrochemistry and forms a fairly good glass matrix at low temperatures for ESR measurements. Additionally, the investigated porphyrins and the potassium salt utilized to induce dimerization of the crown ether porphyrins, potassium tetrakis(4-chlorophenyl)borate, are soluble in this solvent. Hence, all of the physicochemical investigations could be performed in one convenient solvent/electrolyte medium.

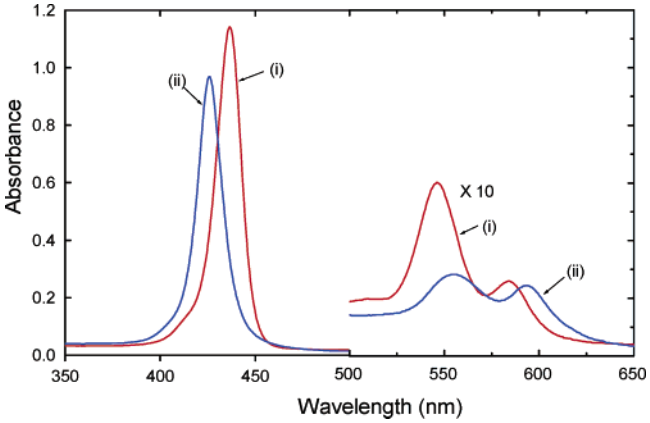

Figure 1. Absorption spectra of (i) AgTCP and (ii) AgTCP + K^+ complex in benzonitrile at room temperature.

UV−Visible Spectral Studies. The optical absorption spectra of the synthesized crown ether porphyrin and its metal derivatives exhibited the characteristic Soret and visible bands. Addition of potassium tetrakis(4-chlorophenyl)borate induced dimerization of the crown ether porphyrins, according to eq 1, revealed by the red shifted visible bands and blue shifted Soret band as a result of exciton coupling.[22] Figure 1 shows the representative spectral changes observed in the case of AgTCP in the absence and presence of added potassium salt, while Table 1 lists the optical data for all of the investigated monomers and potassium ion induced dimers. The dimerization-induced spectral shift in cm^{-1} of the Soret, the most intense visible band, and the radii of the metal ion in the porphyrin cavity are also listed in Table 1. It may be mentioned here that the binding constant, *K*, reported earlier for the dimerization reaction was ∼10^{23} L^5

(20) Lindsey, J. S.; Woodford, J. N. *Inorg. Chem.* **1995**, *34*, 1063.
(21) Frisch, M. J.; Trucks, G. W.; Schlegel, H. B.; Scuseria, G. E.; Robb, M. A.; Cheeseman, J. R.; Montgomery, J. A., Jr.; Vreven, T.; Kudin, K. M.; Burant, J. C.; Millam, J. M.; Iyengar, S. S.; Tomasi, J.; Barone, V.; Mennucci, B.; Cossi, M.; Scalmani, G.; Rega, N.; Petersson, G. A.; Nakatsuji, H.; Hada, M.; Ehara, M.; Toyota, K.; Fukuda, R.; Hasegawa, J.; Ishida, M.; Makajima, T.; Honda, Y.; Kitao, O.; Makai, H.; Klene, M.; Li, X.; Knox, J. E.; Hratchian, H. P.; Cross, J. B.; Adamo, C.; Jaramillo, J.; Gomperts, R.; Stratmann, R. E.; Yazyev, O.; Austin, A. J.; Cammi, R.; Pomelli, C.; Ochterski, J. E.; Ayala, P. Y.; Morokuma, K.; Voth, G. A.; Salvador, P.; Dammenberg, J. J.; Zakrzewski, V. G.; Kapprich, S.; Daniels, A. D.; Strain, M. C.; Farks, O.; Malick, K. D.; Rabuck, A. D.; Raghavachari, K.; Foresman, J. B.; Ortiz, J. V.; Cui, Q.; Baboul, A. G.; Clifford, D. J.; Ciosloski, J.; Stefanoy, B. B.; Liu, G.; Liashenko, A.; Piskorz, P.; Komaromi, I.; Martin, R. L.; Fox, D. J.; Keith, T.; Al-Laham, M. A.; Peng, C. Y.; Nanayakkara, A.; Challacombe, M.; Gill, P. M. W.; Johnson, B.; Chen, W.; Wong, M. W.; Gonzalez, C.; Pople, J. A. *Gaussian 03*, revision B-04; Gaussian, Inc.: Pittsburgh, PA, 2003.
(22) (a) Kasha, M.; Rawls, H. R.; El-Bayoumi, M. A. *Pure Appl. Chem.* **1965**, *11*, 371. (b) Ribó, J. M.; Bofill, J. M.; Crusats, J.; Rubires, R. *Chem.—Eur. J.* **2001**, *7*, 2733.

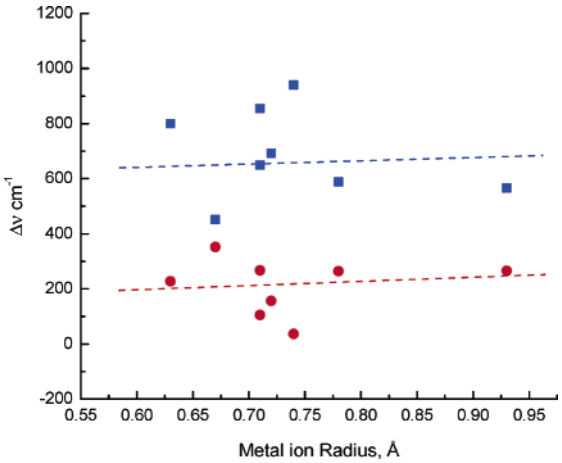

Figure 2. Plot of dimerization-induced spectral shift, $\Delta\bar{\nu}$, cm^{-1}, vs ionic radii, Å, of the central metal ion of the investigated crown ether appended porphyrins for the Soret (■) and the most intense visible (●) bands.

mol^{-1},[3,4] indicating very stable supramolecular complex formation.

$$2P + 4K^+ \rightarrow (K^+)_4(P)_2 \qquad (1)$$

An examination of the data in Table 1 suggests that the observed blue shift of the Soret band varies between 454 and 939 cm^{-1} and compares with a 123−317 cm^{-1} red shift of the most intense visible band (excluding free-base TCP) of the investigated series of compounds. A plot of the spectral shift vs ionic radii resulted in no specific trends and yielded an almost horizontal line (Figure 2) suggesting a minimum influence on the spectral shifts. These results suggest that, to a large extent, the spectral shifts are independent of the metal ion in the porphyrin cavity and more likely are governed by the inter-ring distance between the two interacting porphyrin π-macrocycles which in turn is controlled by the four potassium−bis(crown ether) complexes (vide infra).

Ab Initio DFT Computational Studies. To gain insight into the geometry and electronic structure of MTCP and $K_4(MTCP)_2$, computational studies were performed on a representative ZnTCP and its cation-induced dimer, $K_4(ZnTCP)_2$, by using the B3LYP density functional method (DFT) with a mixed basis set of 3-21G(*) on Zn, K, O, and N atoms and STO-3G on C and H atoms. It should be noted here that the (*) portion of the 3-21G(*) basis set nomenclature is indicative of the fact that d type polarizing functions are not placed on period I atoms. Thus, in the investigated monomer and dimer, only zinc and potassium ions have the d type polarizing functions. DFT methods were chosen over the Hartree−Fock (HF) or semiempirical AM1 or PM3 (PM5) methods since recent studies performed by us on several porphyrin and fullerene bearing molecular and supramolecular systems have revealed that the B3LYP/3-21G(*) method predicts both geometry and electronic structure better than other methods.[24] Using this method, we successfully correlated the computed HOMO and LUMO of the molecular/supramolecular systems to the sequence of the site of electron transfer as determined by electrochemical and spectroelectrochemical methods. Additionally, this computational method has also predicted the geometry of the self-assembled supramolecules formed either by coordination bond, hydrogen bond, or complimentary base-pairing in previous studies.[24] The presently investigated cation-induced crown ether appended porphyrin dimerization presents another interesting example to verify the validity of this low-level ab initio computational procedure to predict the geometry and electronic structure of large supramolecular complexes investigated here.

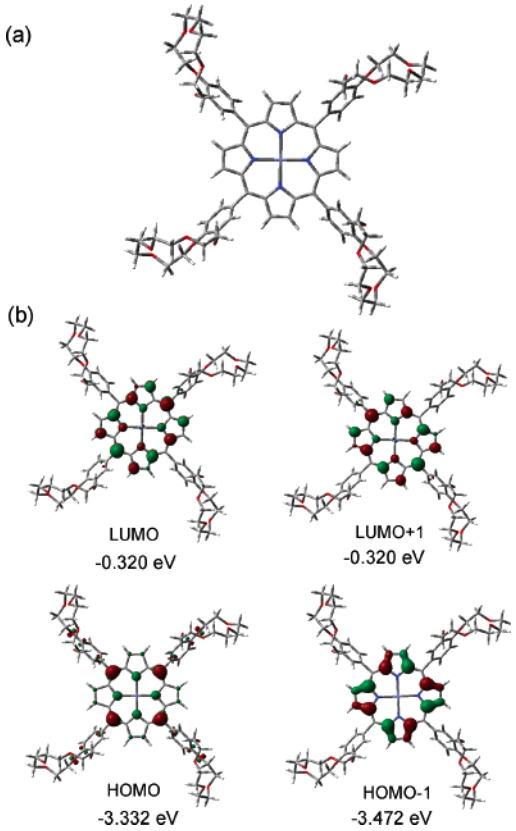

Figure 3. (a) Ab initio B3LYP/(3-21G(*), STO-3G) optimized structure of ZnTCP. (b) B3LYP/(3-21G(*), STO-3G) calculated coefficients of the ZnTCP frontier LUMO, LUMO+1, HOMO, and HOMO-1 orbitals.

Figure 3 shows the optimized structure of the ZnTCP monomer and the four Gouterman's frontier π-orbitals. In the present calculations, the porphyrin monomer and dimer were optimized to a stationary point on the Born−Oppenheimer potential energy surface at the B3LYP/(3-21G(*),

(23) Shannon, R. D. *Acta Crystallogr.* **1976**, *A32*, 751.
(24) (a) D'Souza, F.; Zandler, M. E.; Deviprasad, G. R.; Kutner, W. *J. Phys. Chem. A* **2000**, *104*, 6887. (b) D'Souza, F.; Zandler, M. E.; Smith, P. M.; Deviprasad, G. R.; Arkady, K.; Fujitsuka, M.; Ito, O *J. Phys. Chem. A* **2002**, *106*, 649. (c) Zandler, M. E.; Smith, P. M.; Fujitsuka, M.; Ito, O.; D'Souza, F. *J. Org. Chem.* **2002**, *67*, 9122. (d) Marczak, R.; Hoang, V. T.; Noworyta, K.; Zandler, M. E.; Kutner, W.; D'Souza, F. *J. Mater. Chem.* **2002**, *12*, 2123. (e) D'Souza, F.; Deviprasad, G. R.; Zandler, M. E.; Hoang, V. T.; Klykov, A.; VanStipdonk, M.; Perera, A.; El-Khouly, M. E.; Fujitsuka, M.; Ito. O. *J. Phys. Chem. A* **2002**, *106*, 3243. (f) D'Souza, F.; Deviprasad, G. R.; Zandler, M. E.; El-Khouly, M. E.; Fujitsuka, M.; Ito. O. *J. Phys. Chem. A* **2003**, *107*, 4801. (g) El-Khouly, M. E.; Rogers, L. M.; Zandler, M. E.; Suresh, G.; Fujitsuka, M.; Ito, O.; D'Souza, F. *ChemPhysChem* **2003**, *4*, 474. (h) D'Souza, F.; Smith, P. M.; Zandler, M. E.; McCarty, A. L.; Itou, M.; Araki, Y.; Ito, O. *J. Am. Chem. Soc.* **2004**, *126*, 7898. (i) D'Souza, F.; Smith, P. M.; Gadde, S.; McCarty, A. L.; Kullman, M. J.; Zandler, M. E.; Itou, M.; Araki, Y.; Ito, O. *J. Phys. Chem. B* **2004**, *108*, 11333.

STO-3G) level. No symmetry was imposed. Optimization at the low level was needed in this study because of the large size of the investigated compounds exceeded the orbital limitation of the GAUSSIAN-03 (revision B-04) program used on our Windows PCs. In the optimized structure, the porphyrin ring of the ZnTCP monomer was almost flat with the zinc ion at the center of the ring while the four 15-crown-5 entities were distorted due to the nonlinear geometry of the ethylene oxide groups (Figure 3a). The HOMO and HOMO-1 of the porphyrin ring were a_{2u} and a_{1u} type, respectively (under D_{4h} geometry of the porphyrin ring); that is, for the HOMO the majority of the orbital coefficients were on the four nitrogens and *meso* carbons while, in the HOMO-1, the orbital coefficients were on the α- and β-pyrrole carbon atoms of the porphyrin ring (Figure 3b).[25] The HOMO was also extended to some extent on the benzo-15-crown-5 entities. The LUMO and LUMO+1 were degenerate orbitals, in which the majority of the orbital coefficients were on the porphyrin π-system. The B3LYP/(3-21G(*), STO-3G) calculated HOMO−LUMO energy gap was found to be 3.025 eV.

The tube and space-filling views of the optimized structure of the potassium cation induced ZnTCP dimer, $K_4(ZnTCP)_2$, are shown in Figure 4. In this structure, the two porphyrin rings are stacked with a Zn−Zn distance of 3.9 Å and inter-ring N−N distance of 4.2 Å. The two porphyrin rings lying on top of each other were found to be rotated with respect to one another with N−Zn−Zn−N dihedral angle of 8.9°. Earlier, a 10−45° rotation was envisioned by a CPK space-filling model for a necessary accommodation of the cations in the lateral position.[4] The structure of the potassium ion complexed bis(benzo-15-crown-5 entities were found to be close to that of the structure of potassium bis benzo-15-crown-5) complex reported in the literature.[26] That is, the non-coplanar 15-crown-5 entities become almost coplanar upon binding to potassium. The inter-ring distance between the two crown ether entities was found to be 3.5 Å and compares with a value of 3.4 Å found in the crystal structure of a potassium bis(benzo-15-crown-5) complex.[26]

Interestingly, the calculated HOMO's and LUMO's for the cation-induced dimer were all π-orbitals and degenerate (Figure 4b,c). As predicted for the closely interacting π-systems,[27] the orbital coefficients were nearly equally localized over both of the porphyrin rings. Such a prediction of delocalization of the frontier orbitals on both of the porphyrin macrocycles is an important observation for understanding the electrochemical behavior of the cation-induced MTCP dimers (vide infra). The B3LYP/(3-21G(*), STO-3G) calculated HOMO−LUMO energy gap for $K_4(ZnTCP)_2$ was found to be 3.007 eV.

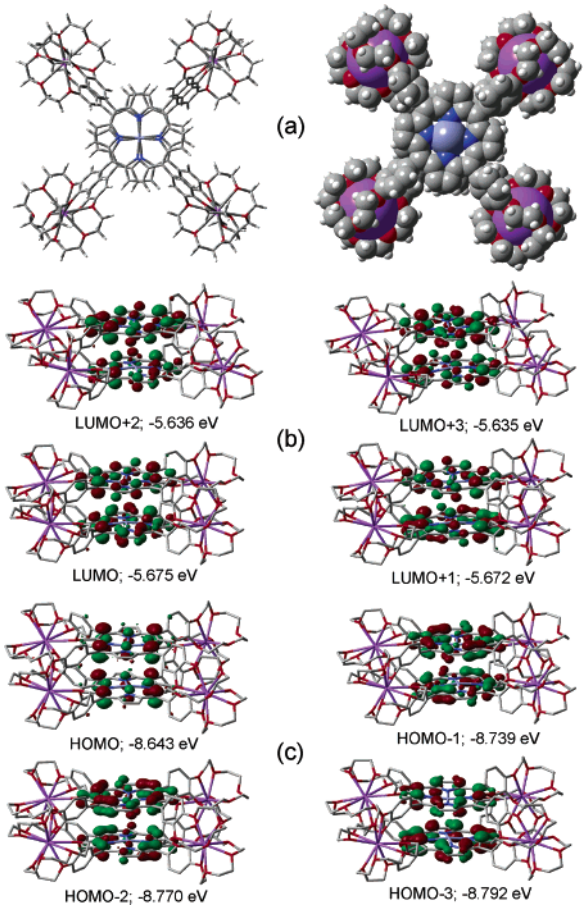

Figure 4. (a) Tube and space-filling models of the ab initio B3LYP/(3-21G(*), STO-3G) optimized structure of potassium ion induced ZnTCP dimer, $K_4(ZnTCP]_2$. (b) and (c) represent B3LYP/(3-21G(*), STO-3G) coefficients of the frontier LUMO, LUMO+1, LUMO+2, LUMO+3, HOMO, HOMO−1, HOMO−2, and HOMO−3 orbitals of the dimer.

ESR Studies. ESR spectroscopy has been widely utilized for characterizing paramagnetic metalloporphyrins, porphyrin π-cation, and π-anion radical species.[28] The existence of metal−metal interactions between the two paramagnetic centers of the porphyrin dimers and aggregates has been studied by using this technique. Earlier, the monomers and cation-induced dimer species of CuTCP and VOTCP were characterized by ESR and ENDOR techniques.[3−6] From these studies, the Cu−Cu and V−V distances measured were found to be ∼4.2 and ∼4.7 Å, respectively. The greater distance in the VOTCP dimer was attributed to the displacement of V from the plane of the porphyrin by ∼0.3 Å as revealed by the X-ray structural studies of vanadyl tetraphenylporphyrin.[29] In this study, we have characterized the newly synthesized paramagnetic complex, AgTCP, and its potassium ion induced dimer by ESR technique. For comparison

(25) Gouterman, M. *The Porphyrins*; Dolphin, D., Ed.; Academic Press: London, 1978; Vol III, pp 1−165.
(26) Mallinson, P. R.; Trutter, M. R. *J. Chem. Soc., Perkin Trans. 2* **1972**, 1818.
(27) (a) Foresman, J. B.; Frisch, A. *Exploring Chemistry with Electronic Structure Methods*; Gaussian Inc.: Pittsburgh, PA, 1993. (b) Hehre, W. J.; Shusterman, A. J.; Nelson, J. E. *The Molecular Modeling Workbook for Organic Chemistry*; Wavefunction, Inc.: Irvine, CA, 1998.
(28) (a) Manoharan, P. T.; Rogers, M. T. In *Electron Spin Resonance of Metal Complexes*; Yen, T. F., Ed.; Plenum Press: New York, 1969. (b) Subramanian, J. In *Porphyrins and Metalloporphyrins*; Smith, K. M., Ed.; Elsevier: Amsterdam, 1975; Chapter 13. (c) Fajer, J.; Davis, M. S. *The Porphyrins*; Dolphin, D., Ed.; Academic Press: London, 1978; Vol. IV, Chapter 4. (d) Sato, M.; Kwan, T. *Bull. Chem. Soc. Jpn.* **1974**, *47*, 1353. (e) Gale, R.; McCaffery, A. J.; Rowe, M. D. *J. Am. Chem. Soc.* **1961**, *83*, 1607.
(29) Chasteen, N. D.; Belford, R. L. *Inorg. Chem.* **1970**, *1*, 169.

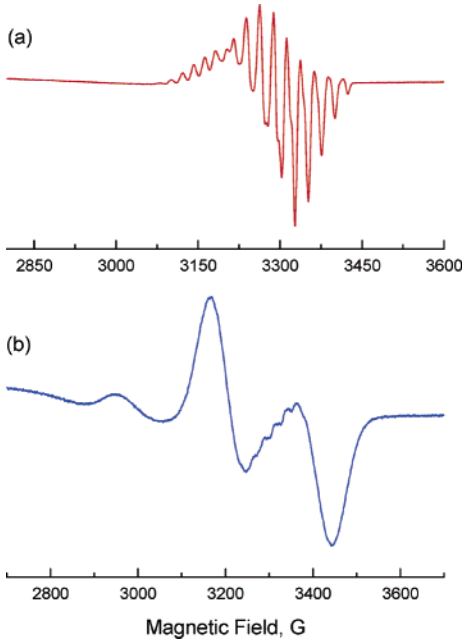

Figure 5. ESR spectra of (a) AgTCP and (b) AgTCP + K^+ complex in benzonitrile at 120 K.

purposes, the CuTCP and VOTCP and their dimers in benzonitrile solvent were also studied.

Figure 5a exhibits the ESR spectrum of AgTCP in benzonitrile at 120 K. The ESR spectrum of AgTCP exhibited splitting of the hyperfine lines due to the interaction of the unpaired electron with the ^{107}Ag and ^{109}Ag nuclear spins ($I = {}^1/_2$) and with the four nitrogens of the porphyrin ring. The g values were calculated according to literature methods.[28e] The spectral behavior for CuTCP and VOTCP were found to be similar to that reported earlier in a toluene matrix.[3−6] That is, they displayed two sets of spectral features corresponding to the parallel and perpendicular alignment of the metalloporphyrin with an axial symmetry (see Supporting Information for spectra). The g and nuclear hyperfine constants calculated according to literature methods[28] are given in Table 2 and were found to be not significantly different from the literature values.[3−6]

The ESR spectrum of $K_4(AgTCP)_2$ obtained by the addition of potassium tetrakis(4-chlorophenyl)borate to the AgTCP benzonitrile solution is shown in Figure 5b while the spectra of $K_4(CuTCP)_2$ and $K_4(VOTCP)_2$ are shown in the Supporting Information. The spectral features for all of the dimers were characteristic of a triplet state with an axial symmetry. Half-field signals corresponding to the $\Delta M_s = \pm 2$ transitions were also observed. In the case of $K_4(AgTCP)_2$, the high-field of the parallel component was superimposed on that of the perpendicular components. No hyperfine structures were observed. The calculated g values were close to the monomer, suggesting the structure of the dimer is similar to that of the monomer. To our knowledge this is the first triplet EPR spectrum of a silver porphyrin dimer. The measured zero field splitting parameter, D, was found to be 256 G for $K_4(AgTCP)_2$, which was lower than that obtained for either of $K_4(CuTCP)_2$ (D = 387 G) or $K_4(VOTCP)_2$ (D = 301 G) under similar experimental conditions. The D values were utilized to evaluate the distance between the two interacting paramagnetic metal ions according to eq 2.[29]

$$R = [3/4g^2\beta^2(1 - \cos^2\theta/D)]^{1/3} \sim (0.65g^2/D)^{1/3} \qquad (2)$$

The measured M−M distances for $K_4(CuTCP)_2$, $K_4(VOTCP)_2$, and $K_4(AgTCP)_2$ were found to be ∼4.2, ∼4.4, and ∼4.8 Å, respectively (Table 2). A higher distance between the interacting Ag−Ag ions is conceivable since X-ray crystallographic studies[30] of Ag porphyrin have shown that the Ag^{II} ion is out of the plane of the porphyrin ring. In this context it may be mentioned that the Cu in Cu porphyrin is almost at the center of the ring while the V in VO porphyrin is out of plane by ∼0.3 Å and, hence, the trend in the M−M distances. It is interesting to note that the optical absorption spectral studies revealed no specific trends in their spectral shifts with respect to the metal ion radius while the M−M distances measured from ESR were found to be sensitive to the metal ions. As pointed out earlier, in the dimers held by four potassium bis(15-crown-5) complexes, the inter-ring distance and the resulting spectral shifts (originated from the ring $\pi-\pi$ transitions) are fairly constant, and the influence of the central metal ion in the porphyrin cavity is minimum.

Electrochemical Studies. The electrochemical behavior of the MTCPs and their cation-induced dimers was investigated using both cyclic voltammetry (CV) and differential pulse voltammetry (DPV). The peak currents and peak potentials were found to be better defined in DPV than in CV experiments. Hence, in the present discussions the DPV results are utilized. Figure 6 shows representative DPVs for the monomer and potassium cation induced dimers in benzonitrile, 0.1 M $(TBA)ClO_4$. The peak potentials and the electrochemically calculated HOMO−LUMO gaps, that is, the potential difference between the first oxidation and reduction, are given in Table 3.

A large irreversible anodic wave was observed for all of the investigated MTCPs upon scanning the potential beyond the first oxidation, presumably due to the oxidation of the crown ether entities. Independent experiments performed on benzo-15-crown-5 also revealed such an irreversible anodic

Table 2. ESR Data for MTCP and $K_4(MTCP)_2$ (M = Cu, VO, Ag) in Benzonitrile at 120 K

compd	$g_{\|}$	$g_\perp$	$10^{-4}A_{\|}^M$, cm^{-1}	$10^{-4}A_\perp^M$, cm^{-1}	D, G	R, Å
CuTCP	2.157	2.004	201	32		
$K_4(CuTCP)_2$	2.153	1.998	98		387	4.24
VOTCP	1.990	1.993	168	60		
$K_4(VOTCP)_2$	1.977		85		301	4.38
AgTCP	2.063	1.995				
$K_4(AgTCP)_2$	2.074	2.008			256	4.78

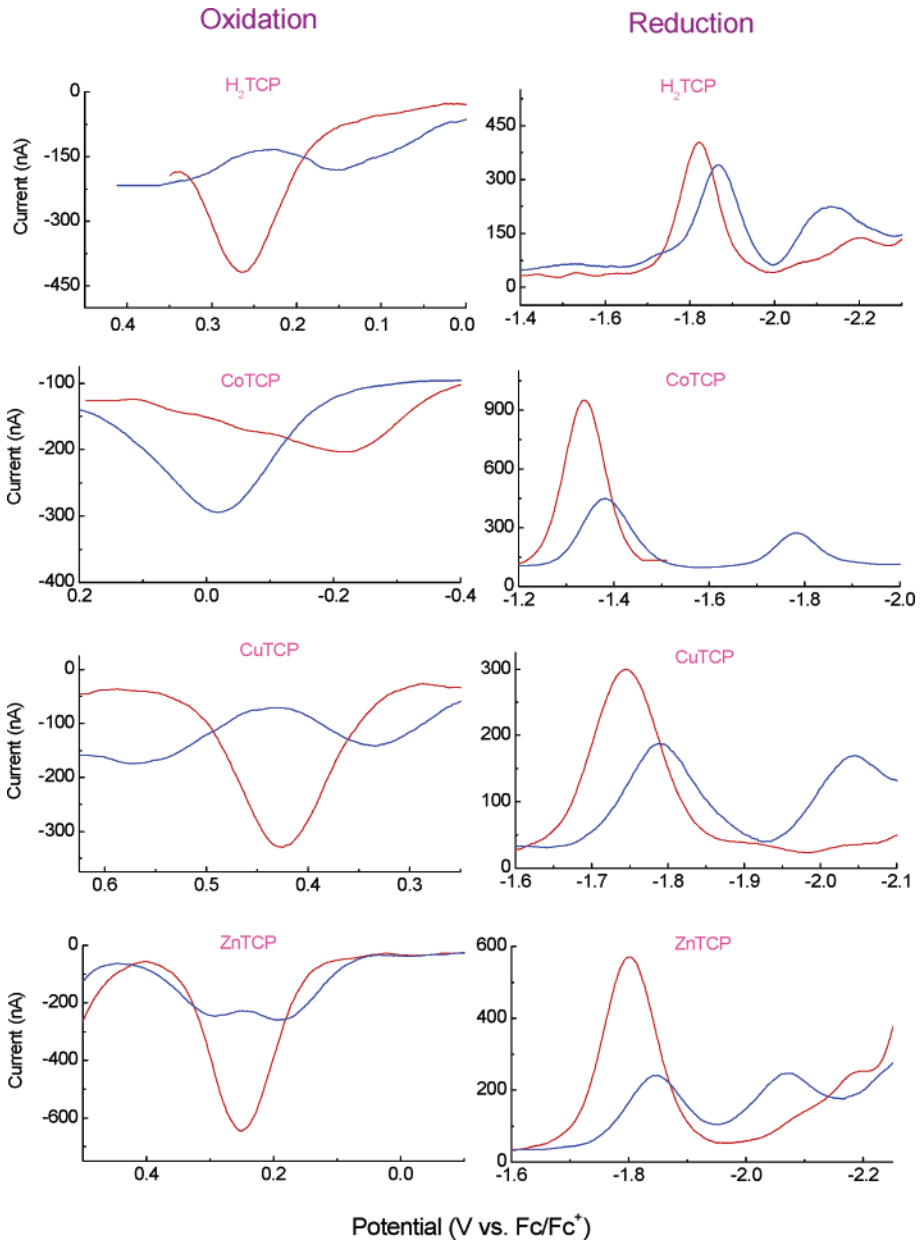

Figure 6. Differential pulse voltammograms of H_2TCP, CoTCP, CuTCP, and ZnTCP (~0.5 mM, red line) and their potassium cation induced dimers (blue line) in benzonitrile, 0.1 M $(TBA)ClO_4$. The concentration of potassium tetrakis(4-chlorophenylborate) used to induce dimerization was ~10 mM. Scan rate = 5 mV/s, pulse width = 0.25 s, and pulse height = 0.025 V.

wave. Therefore, it was only possible to monitor the first oxidation process. Control experiments suggested that the first oxidation is a reversible one-electron process, except for CoTCP, where an irreversible metal centered $Co^{II/III}$ process was observed by both DPV and CV. Scanning the potential on the cathodic side exhibited one or two reversible reductions for all of the studied MTCPs. The peak potentials of the first oxidation and the first reduction were utilized to establish the HOMO−LUMO energy level diagram in Figure 7.

Addition of potassium ions to the MTCP solution revealed interesting observations. Except for CoTCP, all of the MTCP dimers revealed a cathodic shift and the currents were approximately half of that recorded for the MTCP monomers. When the the potential was scanned further in the anodic direction, an additional wave just before the large irreversible anodic wave was observed. Interestingly, the currents for the second waves were similar in magnitude to that of the first oxidation. That is, splitting of the oxidation waves were observed for all of the dimers, a result that is expected for two interacting porphyrin macrocycles[31] and as predicted earlier from the frontier HOMO and LUMO orbital calculations where extensive delocalization of the orbitals were observed on both the porphyrin rings. The potential difference between these two peaks is indicative of the extent of interaction between the porphyrin rings in the dimer. In the absence of such interactions one would expect only a single

(30) (a) Hoard, J. L. In *Porphyrins and Metalloporphyrins*; Smith, K. M., Ed.; Elsevier: Amsterdam, 1975; Chapter 8. (b) Molinaro, F. S.; Ibers, J. A. *Inorg. Chem.* **1976**, *15*, 2279.

(31) Shultz, D. A.; Lee, H.; Kumer, R. K.; Gwaltney, K. P. *J. Org. Chem.* **1999**, *64*, 9124.

Table 3. Redox Potentials (V) Determined from Differential Pulse Voltammetry[a] for the Crown Ether Appended Porphyrins and Their Potassium Ion Induced Dimers in Benzonitrile, 0.1 M $(TBA)ClO_4$

compd	2nd oxdn	1st oxdn	1st redn	2nd redn	$E_{oxdn} - E_{redn}$, V
TCP		0.264	−1.822	−2.20	2.086
TCP + K^+		0.155	−1.869	−2.13	2.024
MgTCP		0.123	−1.923	−2.11	2.046
MgTCP + K^+	0.667	0.144	−1.892	−2.072	2.036
VOTCP		0.557	−1.58	−1.776	2.137
VOTCP + K^+		0.391	−1.542	−1.731	1.933
CoTCP		−0.218	−1.338		*b*
CoTCP + K^+		−0.02	−1.381	−1.784	*b*
NiTCP		0.555	−1.693		2.248
NiTCP + K^+	0.398	0.265	−1.801	−2.037	2.066
CuTCP		0.427	−1.744		2.171
CuTCP + K^+	0.588	0.335	−1.790	−2.043	2.125
ZnTCP		0.253	−1.802		2.055
ZnTCP + K^+	0.294	0.184	−1.847	−2.069	2.031
PdTCP		0.607	−1.684		2.291
PdTCP + K^+		0.419	−1.789	−2.080	2.208
AgTCP		0.038	−1.447	−1.640	*b*
AgTCP + K^+	0.149	0.008	−1.484	−1.740	*b*

[a] Scan rate = 5 mV/s, pulse width = 0.25 s, and pulse height = 0.025 V. [b] Metal-centered oxidation or reduction process.

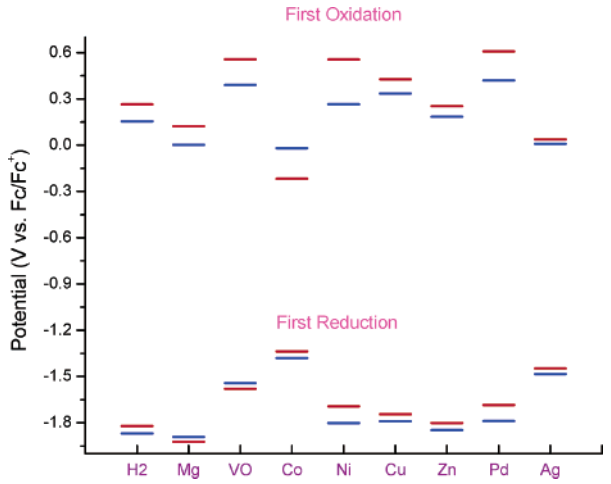

Figure 7. Electrochemically measured HOMO and LUMO energy levels of the monomer, MTCP (red line), and dimer, $K_4(MTCP)_2$ (blue line), crown ether appended porphyrins. M = H_2, Mg, VO, Co, Ni, Cu, Zn, Pd, and Ag.

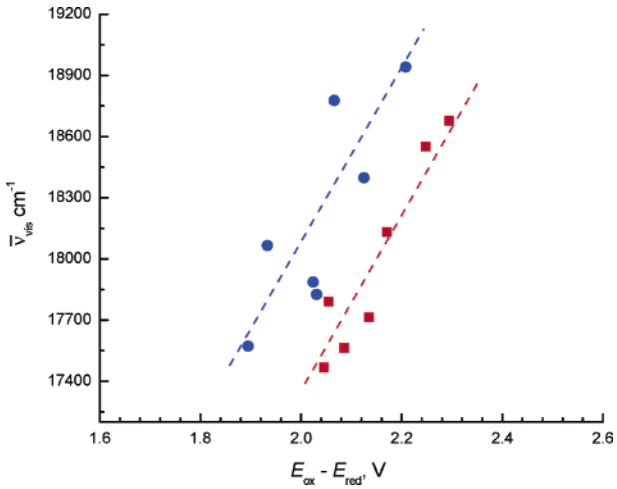

Figure 8. Plot of $\Delta\bar{\nu}_{vis}$, cm^{-1} (for the most intense visible band), vs electrochemically measured HOMO−LUMO gap as $E_{ox} - E_{red}$ for the investigated series of monomer, MTCP (red line), and dimer, $K_4(MTCP)_2$ (blue line), porphyrins.

wave corresponding to the oxidation process of the dimer. It may be mentioned here that reduced peak currents for the dimers might also occur due to the lower diffusion coefficient of the dimers; however, such an effect would not reduce the current to half the initial value. In the strongly interacting dimers, during the oxidation or reduction process, only half of the molecule, that is, one of the porphyrin rings of the dimer, is expected to undergo an initial electrochemical process followed by the second porphyrin ring. As shown in Figure 6, this trend also follows for the reduction process of all of the MTCPs. A split reduction wave was observed for all of the investigated metalloporphyrin dimers (Table 3).

Figure 7 shows the HOMO−LUMO energy level diagram constructed using the electrochemical data for both monomers and dimers. It is clear from the results that the HOMO of the porphyrin dimer is destabilized while the LUMO is stabilized, and such a perturbation is more for the HOMO energy level than for the LUMO energy level. The overall effect of this is a reduced HOMO−LUMO gap and subsequent red-shifted Q-bands. This effect is illustrated in Figure 8 in which the energy of the most intense visible band is plotted against the electrochemically measured HOMO−LUMO gap for both the monomers and the dimers. Linear trends for both the plots were observed indicating a good agreement of the energies between the two measurements of the porphyrin monomers and dimers. It may be mentioned here that the B3LYP/(3-21G(*), STO-3G) computed HOMO−LUMO gap of ZnTCP and $K_4(ZnTCP)_2$ was 3.025 and 3.007 eV, respectively, which compared with the electrochemically measured energy gap of 2.055 and 2.031 V, respectively. It may be mentioned here that a time-dependent DFT (TD DFT) calculation at the B3LYP/(3-21G(*), STO-3G) level of the singlet−singlet transition of the monomer yielded a value of ∼2.40 eV, in much better agreement with the observed electrochemical gap of 2.055 V. The net change in energy between the ZnTCP and $K_4(ZnTCP)_2$ was 0.015 eV by computational calculations which agreed fairly well

with the electrochemically measured value of 0.024 V. A reduced HOMO−LUMO gap for the dimer was predicted by the computational calculations, and this prediction was confirmed by the experimental results obtained from the optical absorption and electrochemical studies.

Summary. 5,10,15,20-Tetrakis(benzo-15-crown-5)porphyrin (TCP) and a series of metal derivatives (MTCP; M = Mg(II), VO(IV), Co(II), Ni(II), Cu(II), Zn(II), Pd(II), Ag(II)) were synthesized and characterized by spectroscopic and B3LYP/3-21G(*) methods. Differential pulse voltammetry was utilized to probe the effect of the potassium ion induced dimerization of the porphyrins on the oxidation and reduction potentials. The HOMO−LUMO energy level diagram constructed from the electrochemical data revealed destabilization of the HOMO level and stabilization of the LUMO level upon dimer formation. The ab initio B3LYP/(3-21G(*), STO-3G) method was employed to visualize the geometry and electronic structure of ZnTCP and its dimer, $K_4(ZnTCP)_2$. The computed inter-porphyrin ring distance of the dimer agreed well with the spectroscopically determined values, and the calculated frontier HOMO and LUMO orbitals revealed extensive delocalization on both of the porphyrin rings. The computational calculations also predicted a smaller HOMO−LUMO gap for the dimer, and this prediction was confirmed by the results of optical absorption and electrochemical studies. ESR spectroscopy was utilized to investigate the paramagnetic porphyrins and their dimers. The ESR spectra of the dimers resulted in a triplet state owing to the interaction between the two paramagnetic centers. The metal−metal distances calculated from ESR method followed the trend Cu−Cu < VO−VO < Ag−Ag. Good correlations between the electrochemically measured HOMO−LUMO gap and energy corresponding to the most intense visible band of both MTCP and $K_4(MTCP)_2$ were observed.

Acknowledgment. The authors are thankful to the donors of the Petroleum Research Fund, administered by the American Chemical Society, and National Institutes of Health (Grant GM 59038 to F.D.) for support of this work. L.M.R. is thankful to the Department of Education for a GAANN fellowship. P.A.K. is thankful to the NSF for a RSEC fellowship.

Note Added in Proof: While this manuscript was in press, the ZnTCP and $K_4(ZnTCP)_2$ were optimized at the B3LYP/3-21G(*) level on a newly available SGI Altix 3700 with 32 Itanium-2 processors. The geometry and electronic structures were found to be not significantly different from the B3LYP/(3-21G(*), STO-3G) calculations reported in the manuscript. The B3LYP/3-21G(*) calculated HOMO−LUMO gaps were found to be 2.94 and 2.90 eV, respectively, for ZnTCP and $K_4(ZnTCP)_2$.

Supporting Information Available: ESR spectra of the monomer and dimer of CuTCP and VOTCP. This material is available free of charge via the Internet at http://pubs.acs.org.

IC0497228